IN VIVO PECTORALIS MUSCLE FORCE–LENGTH BEHAVIOR DURING LEVEL FLIGHT IN PIGEONS (*COLUMBA LIVIA*)

ANDREW A. BIEWENER[1],[*],[‡], WILLIAM R. CORNING[1] AND BRET W. TOBALSKE[2],[‡]

[1]*Department of Organismal Biology and Anatomy, The University of Chicago, 1027 E. 57th St., Chicago, IL 60637, USA* and [2]*Division of Biological Sciences, University of Montana, Missoula, MT 59812, USA*

[*]e-mail: abiewener@oeb.harvard.edu

[‡]Present address: Concord Field Station, Museum of Comparative Zoology, Department of Organismic and Evolutionary Biology, Harvard University, Old Causeway Road, Bedford, MA 02130, USA

Summary

For the first time, we report *in vivo* measurements of pectoralis muscle length change obtained using sonomicrometry combined with measurements of its force development *via* deltopectoral crest strain recordings of a bird in free flight. These measurements allow us to characterize the contractile behavior and mechanical power output of the pectoralis under dynamic conditions of slow level flight in pigeons *Columba livia*. Our recordings confirm that the pigeon pectoralis generates *in vivo* work loops that begin with the rapid development of force as the muscle is being stretched or remains nearly isometric near the end of the upstroke. The pectoralis then shortens by a total of 32 % of its resting length during the downstroke, generating an average of $10.3\pm3.6\,\mathrm{J\,kg^{-1}}$ muscle (mean ± S.D.) of work per cycle for the anterior and posterior sites recorded among the five animals. In contrast to previous kinematic estimates of muscle length change relative to force development, the sonomicrometry measurements of fascicle length change show that force declines during muscle shortening. Simultaneous measurements of fascicle length change at anterior and posterior sites within the same muscle show significant ($P<0.001$, three of four animals) differences in fractional length (strain) change that averaged 19±12 %, despite exhibiting similar work loop shape. Length changes at both anterior and posterior sites were nearly synchronous and had an asymmetrical pattern, with shortening occupying 63 % of the cycle. This nearly 2:1 phase ratio of shortening to lengthening probably favors the ability of the muscle to do work. Mean muscle shortening velocity was 5.38 ± 1.33 and $4.88\pm1.27\,\mathrm{lengths\,s^{-1}}$ at the anterior and posterior sites respectively. Length excursions of the muscle were more variable at the end of the downstroke (maximum shortening), particularly when the birds landed, compared with highly uniform length excursions at the end of the upstroke (maximum lengthening). When averaged for the muscle as a whole, our *in vivo* work measurements yield a mass-specific net mechanical power output of $70.2\,\mathrm{W\,kg^{-1}}$ for the muscle when the birds flew at 5–$6\,\mathrm{m\,s^{-1}}$, with a wingbeat frequency of 8.7 Hz. This is 38 % greater than the value that we obtained previously for wild-type pigeons, but still 24–50 % less than that predicted by theory.

Key words: pigeon, *Columba livia*, muscle, force–length behavior, flight, sonomicrometry, pectoralis, mechanical power output.

Introduction

The performance of birds in flight has long fascinated biologists and aerodynamicists. Understanding the neural and musculoskeletal bases of the wing's ability to generate lift is of interest in this regard. In the past, estimates of the mechanical power required for animal flight have largely relied on quasi-steady aerodynamic theory (e.g. Pennycuick, 1968, 1989; Norberg and Rayner, 1987; Norberg, 1990) and classical interpretations of muscle function (Weis-Fogh and Alexander, 1977). While these approaches have yielded considerable insight into the kinematics and the musculoskeletal and aerodynamic features of wing design important to flapping flight, they ignore changes in wing form and the unsteady effects of air flow over the wing that are likely to be important

(Rayner, 1979; Ellington, 1984). Using flow visualization of the vorticity shed in the wake of a flying bird, recent studies have attempted to account for such effects by quantifying the aerodynamic circulation generated by the wing (Spedding *et al.* 1984; Spedding, 1986, 1987; Rayner, 1995). Such measurements suggest that classical aerodynamic theory probably overestimates the power requirements for slow forward flight, but may better describe the requirements for faster flight (Spedding, 1987), when birds fly using a 'continuous vortex gait' (Rayner, 1995). New experimental techniques now also make it possible to record the *in vivo* length changes and forces developed by certain key locomotory muscles during functional activity (Biewener and

Baudinette, 1995; Biewener *et al.* 1992, 1998; Griffiths, 1991; Marsh *et al.* 1992; Roberts *et al.* 1997). These approaches allow muscle function to be studied under dynamic conditions and thus provide a direct means for assessing the mechanical power output of a bird in flight.

Our goal in this paper is to characterize the *in vivo* force and length changes of the pectoralis muscle in order to estimate better the mechanical power output of bird in free flight. Because the pectoralis muscles represent a substantial fraction (combined, 15–20 %) of the bird's body mass (Greenewalt, 1975) and are believed to provide most of the mechanical power required for lift generation during flapping flight (Dial, 1992; Dial and Biewener, 1993), measurements of the pectoralis alone allow a good estimate of the power output of the whole animal. Previous studies have taken advantage of this to examine the mechanical power requirements of starlings (*Sturnus vulgaris*; Biewener *et al.* 1992), pigeons (*Columba livia*; Dial and Biewener, 1993) and, most recently, black-billed magpies (*Pica pica*; Dial *et al.* 1997) during steady forward flight. In these studies, we developed an approach to measure the forces generated by the pectoralis by means of recording *in vivo* strains produced within the deltopectoral crest (DPC) of the humerus, the insertion of the pectoralis on the wing. Our results for starlings and magpies flying in a wind tunnel and for pigeons in free flight suggest that estimates of mechanical power output based on traditional aerodynamic theory are too high. In addition, they show that differences in power requirements for take-off and ascending *versus* level flight may be smaller than previously thought (Dial and Biewener, 1993). Measurements made in magpies over a range of steady speeds, while flying in a wind tunnel (Dial *et al.* 1997), also indicate that classical descriptions of a 'U'-shaped power curve for forward flapping flight can be substantially altered by changes in the flight behavior of a bird over a range of speeds. The use of these measurements to determine muscle work and mechanical power, however, are limited by kinematic estimates of muscle length change based on distal wing kinematics to estimate proximal wing excursion (Scholey, 1983). We now combine our DPC force measurements with direct recordings of *in vivo* muscle length using sonomicrometry to re-examine some of these findings and to describe more fully the dynamic behavior of the muscle during free flight.

In vivo force and muscle length change recordings

considerably broaden our understanding of the dynamic behavior of a muscle as it performs its normal functions. Although the Hill force–velocity relationship (Hill, 1938) successfully describes the behavior of striated muscle in relation to competing demands for force, speed of movement and power output, it represents experimental measurements of force under quasi-static (isotonic and small shortening distances) conditions (McMahon, 1984). Consequently, it is unlikely to reflect the behavior of muscles that must develop force continuously under time-varying conditions of movement and during transient periods of activation.

In this study, we present the first simultaneous recordings of *in vivo* muscle force and length changes in a flying bird, providing cycle-by-cycle measurements of muscle work and power output. The oscillatory nature of animal limb movements produces cycles of muscle shortening and lengthening relative to force production that result in force–length patterns termed muscle 'work loops'. Following the early work of Machin and Pringle (1960) and Josephson (1985), numerous *in vitro* analyses of work loops generated by isolated whole muscles (Marsh and Olson, 1994; Stevens, 1988; Stevenson and Josephson, 1990) or muscle fiber bundles (Altringham and Johnston, 1990; Barclay, 1994; Curtin and Woledge, 1993; Lutz and Rome, 1994; Rome *et al.* 1993) in response to activation during imposed sinusoidal length oscillations have provided valuable information on how stimulation phase, frequency and strain amplitude affect the ability of a muscle to generate mechanical power. Marsh and Olson (1994) have used this approach to begin to study how the *in vivo* dynamics of muscle length change of scallop (*Argopecten irradians*) adductor muscle during jetting affects the *in vitro* force–velocity properties and work performance of the muscle. We take a similar approach to investigate the dynamics of muscle function by examining *in vivo* work loops generated by the pectoralis muscle of pigeons (*Columba livia*) during free flight.

Materials and methods
Animals and training

Five Silver King pigeons (*Columba livia*; mean body mass 649 g, Table 1), a large racing breed, were obtained from a commercial source and trained to fly from hand a short distance (10–12 m) to a perch. The perch consisted of a 0.4 m×0.3 m

Table 1. *Summary of muscle and wing morphology of the experimental pigeons*

Animal	Body mass (kg)	Wing loading (N m^{-2})	Disk loading (N m^{-1})	Fasicle length (mm)				Pectoralis mass (g)
				Anterior	Posterior	Mean ± S.D.	N	
1	0.599	71.2	8.14	65	72	54±11	16	57.9
2	0.668	75.6	9.05	77	64	57±13	17	57.7
3	0.598	68.1	8.04	69	61	48±15	15	50.6
4	0.657	86.0	9.32	77	58	60±14	16	60.5
5	0.638	67.1	8.63	69	60	54±12	14	54.3
Mean ± S.D.	0.649±0.032	7.50±0.79	8.64±0.6	71±5	63±5	55±5		58.2±6.6

platform located 1.2 m above the floor in front of a window to encourage the birds to fly to the perch. The indoor flight path allowed the birds to achieve steady slow level flight (5–6 m s⁻¹) over much of the course. A light nylon string attached to the bird's ankle by means of a soft leather jess prevented it from escaping after being released. Flight training was carried out for 30–45 min per day over a 5 week period prior to conducting experimental recordings.

Surgical procedures

To implant sterilized sonomicrometry muscle length transducers, electromyography (EMG) electrodes and bone strain gauges following the training period, the birds were initially anesthetized with intramuscular injections of ketamine (20 mg kg⁻¹) and xylazine (2 mg kg⁻¹); supplemental doses were administered as needed. Once an appropriate level of anesthesia had been achieved, the feathers over the left shoulder, upper back and left pectoralis (to the base of the keel of the sternum) were removed and the skin surfaces disinfected with betadine solution. After a 3 cm incision had been made over the ventral surface of the pectoralis, a second much smaller opening was made in the skin over the animal's back, so that the EMG and sonomicrometry crystal electrodes could be passed subcutaneously beneath the wing (*via* a short piece of 5 mm i.d. plastic tubing) to the opening over the pectoralis. Two pairs of sonomicrometry crystals and EMG electrodes were used to allow separate length change and EMG measurements to be made in an anterior and posterior location within the sternobrachial (SB) portion of the pectoralis
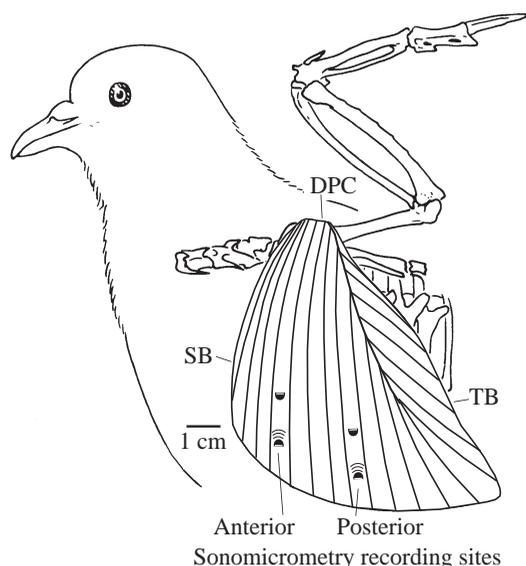

Fig. 1. Lateral view of the left pectoralis showing the anterior and posterior sonomicrometry (and electromyography) electrode recording sites. The pectoralis inserts proximally onto the ventral aspect of the deltopectoral crest (DPC), where strains were measured on its dorsal surface. Electrode lead wires were passed subcutaneously to a small back-plug connector located over the back of the bird between its wings. SB, sternobrachial portion of the pectoralis; TB, thoracobrachial portion of the pectoralis.

(Fig. 1). The anterior recording site was located approximately 15 mm from the anterior border of the muscle where it attaches to the furcula. The posterior site was located approximately 30 mm caudal to the anterior site. At both sites, the muscle fascicles of the sternobrachial portion of the pectoralis run parallel to the superficial surface of the muscle. The anterior fascicles originate from the keel of the sternum and pass directly to the muscle's insertion on the ventral surface of the deltopectoral crest (DPC) of the humerus. The fascicles in the posterior recording site insert into an intramuscular aponeurosis continuous with the muscle's insertion on the ventral DPC. Fascicles in the anterior site are oriented nearly dorsally, while those at the posterior site run at a slightly more anteroposterior angle. In the five birds studied, the angle of the anterior fascicles averaged 82° with respect to the keel of the sternum (defined by its most anterior and posterior points), whereas the posterior fascicles ran at an angle of approximately 75° (Fig. 1). Consequently, in addition to humeral depression, the posterior fascicles may also tend to retract the humerus more than the anterior fascicles.

The avian pectoralis is well suited for making *in vivo* measurements of fascicle length change by means of sonomicrometry because of the parallel organization of the muscle's fibers at its superficial surface. As described in a previous study (Biewener *et al.* 1998), each 2 mm disc sonomicrometry crystal (SL2, Triton, Inc.) was glued using epoxy resin to a stainless-steel wire holder that was bent to provide a support arm with two small loops. This allowed the crystals to be positioned at a depth of approximately 6 mm beneath the surface of the muscle, aligned to the fascicle axis, and anchored with 4-0 gauge silk suture through the wire loops to the superficial fascia of the muscle. In all birds, the crystals were implanted 13–16 mm apart from each other. A small opening parallel to the fascicles was made by puncturing the surface of the muscle and spreading it using small sharp-pointed scissors. After inserting the sonomicrometry crystal, this opening was sutured closed with 4-0 gauge silk. In addition to the sonomicrometry crystal pairs, fine-wire bipolar silver hook EMG electrodes (0.5 mm bared tips with 2 mm spacing, California Fine Wire, Inc.) were implanted immediately adjacent to the anterior and posterior sites to confirm that length change recordings represented activated muscle fibers. The EMG electrodes were inserted at a shallow angle parallel to the fascicle axis using a 23 gauge hypodermic needle and anchored using a 4-0 gauge silk suture at the exit point from the muscle's surface. A second tie was also made further back close to the keel of the sternum with a small loop of wire between the two ties that served as strain relief and helped to reduce movement artifacts in the EMG signal.

Sonomicrometry

Sonomicrometry provides a direct measurement of length change by recording the transit time for an ultrasonic sound pulse that is emitted by one crystal and received by the other of a pair. Because the Triton 120.2 sonomicrometry system assumes a sound velocity of 1500 m s⁻¹, length changes were

corrected by 2.7 % for the velocity of sound in skeletal muscle ($1540\,\mathrm{m\,s^{-1}}$, Goldman and Hueter, 1956; Goldman and Richards, 1954). The Triton 120.2 system also introduces a 5 ms delay in the recorded changes in length between the crystals (Marsh *et al.* 1992). Consequently, length recordings were corrected for this phase delay before analyzing the temporal aspects of muscle activation, length change and force development. Measurements of length change (Δl) are made between the two crystals, with fractional length change (L_{fract}) being determined with reference to the resting distance between the crystals ($L_{\mathrm{fract}}=\Delta l/L_{\mathrm{rest}}$). Resting length ($L_{\mathrm{rest}}$) was defined as the distance between the crystals recorded at the end of the flight sequence, after the bird had landed on the perch with its wings held at its sides (see Fig. 2). Because of the long length of the muscle's fascicles (anterior L_{tot} 71±5 mm, posterior L_{tot} 63±5 mm; means ± S.D.; Table 1), total fascicle length change (ΔL) was calculated as, $\Delta L = L_{\mathrm{fract}} \times L_{\mathrm{tot}}$. Consequently, measurements of ΔL assume uniform length change along the entire length of the fascicle. Following the completion of the experimental recordings, all sonomicrometry crystal implant locations were verified with respect to the fascicle axis on the basis of *post-mortem* dissection. In all cases, the crystals were found to be well aligned (difference $<4\,°$) with the muscle fascicles, rendering alignment errors of muscle length change insignificant.

Deltopectoral crest strain recordings of muscle force

In addition to implanting sonomicrometry and EMG electrodes within the pectoralis, we also attached a single-element metal foil strain gauge (FLE-1, Tokyo Sokki Kenkyujo, Ltd, Japan) to the dorsal surface of the deltopectoral crest (DPC) of the humerus (Fig. 1). This was achieved by making a small (15 mm) incision over the left shoulder and reflecting the overlying deltoid muscle to expose the bony surface of the DPC. The strain gauge and its lead wires were passed subcutaneously and deep to the deltoid muscle to the DPC installation site. After removing the overlying periosteum with a scalpel and drying the bone surface with a cotton applicator dipped in ether, the strain gauge was bonded to the dorsal surface of the DPC, perpendicular to the humeral shaft, using a self-catalyzing cyanoacrylate adhesive. Following our previous studies (Biewener *et al.* 1992; Dial and Biewener, 1993), we used recordings of dorsal DPC strain to quantify pectoralis force generation under *in vivo* flight conditions. During the downstroke, the DPC is pulled ventrally by the contracting pectoralis, so that the dorsal surface develops a principal axis of tensile strain that is nearly perpendicular to the long axis of the humerus. This makes the strain gauge sensitive to forces produced by the pectoralis but not by other muscle or to aerodynamic forces transmitted by the bone between the elbow and the shoulder.

Following implantation of the DPC strain gauge and the muscle electrodes, all the wounds were sutured closed. A miniature back plug, previously soldered to the lead wires of the transducers and insulated prior to surgery, was anchored to the skin and vertebral ligaments using 3-0 gauge silk. The animals were then allowed to recover for 24 h prior to making experimental recordings.

### Flight recordings and calibration procedures

Experimental recordings of pectoralis EMG, fascicle length change and DPC strain were made over the following 2 days. These recordings were made by connecting the animal to a lightweight 12 m shielded cable that the animal dragged behind it as it flew (the suspended portion of the cable weighed approximately 55 g). The cable was connected at the other end to a strain gauge bridge amplifier (Vishay 2120, Micromeasurements), EMG amplifiers (Grass, P-511) and two channels of a Triton 120.2 sonomicrometry amplifier. The output of each of these amplifiers was sampled by an A/D converter at 1000 Hz and stored on a computer for subsequent analysis. At least five successful flights were recorded for each animal. Flights in which the animal did not land on the perch or veered off course were not analyzed.

Video-tape recordings (Panasonic AG450 S-VHS camera equipped with a 10× zoom lens) were obtained (at $60\,\mathrm{fields\,s^{-1}}$) of various flights from the posterior, lateral (midway along the flight path) and anterior views. These recordings were used to determine the animal's body angle during flight and gross aspects of the wing movement. Kinematic data were obtained from digitally acquired video images (played out from a Panasonic AG-1960 deck through an IDEN model IVT-7 time-base correction amplifier to an Imaging Technologies PC-Vision Plus frame-grabbing board) using MTv software (DataCrunch, Inc.) on a Pentium II computer.

After the recordings had been completed, the animal was killed with an overdose of sodium pentobarbitol ($100\,\mathrm{mg\,kg^{-1}}$, intravenously). The relationship between DPC strain and pectoralis muscle force was quantified by attaching the pectoralis to a force transducer using 0 gauge silk suture tied just below the muscle's insertion on the DPC. A series of 'pull' calibrations was then performed with the wing held in three positions of elevation (horizontal, 30 $°$ and 60 $°$ above horizontal) corresponding to the range of motion over which the pectoralis exerts its greatest force. Least-squares linear regressions of the rise and fall of DPC strain *versus* measured force were obtained to achieve a dynamic calibration of pectoralis force. In all cases, regressions had $r^2 > 0.995$, with the differences in slope (hysteresis) for the rise *versus* fall in force being less than 4 %. The calibration slopes obtained at the different orientations were averaged for each bird.

Morphological measurements of pectoralis mass, mean fascicle length (based on 14–17 separate measurements obtained for varying regions of the muscle along both its superficial and deep surfaces, using metric digital calipers), wing loading (body mass divided by projected area of body and wings when fully extended; after Pennycuick, 1989) and disk loading (body mass divided by wing span) were also obtained (Table 1). Unless otherwise noted, values are

Fig. 2. *In vivo* recordings of pectoralis force calibrated from strains measured at the deltopectoral crest (DPC), together with sonomicrometry recordings of fascicle length change and electromographic (EMG) recordings at anterior and posterior sites within the pectoralis muscle of pigeon 1 (see Fig. 1). These recordings were obtained as the bird took off, when released by hand, and flew straight and fairly level before landing on a perch. Characteristic of wing elevation and depression, the muscle exhibits slightly skewed sinusoidal changes in length at both recording sites. The resting length of the muscle's fascicles was determined at the end of the flight sequence (denoted by an arrow) as the bird came to rest with its wings folded against its sides. The shaded wingbeat cycle is shown expanded in Fig. 4.
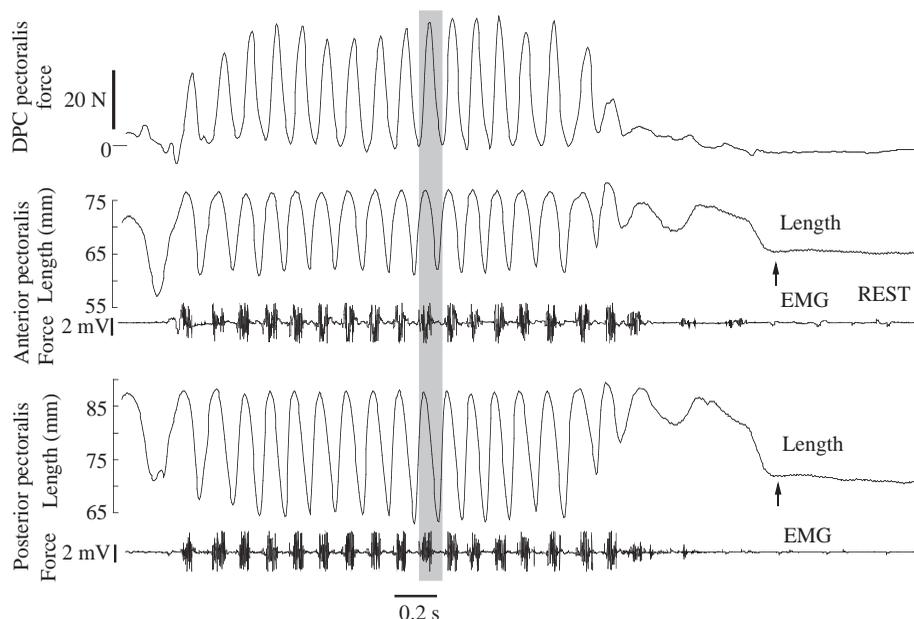
presented as the mean ± S.D., and statistical comparisons among means were carried out using paired *t*-tests.

Results

Flight recordings of muscle force, length and muscle activation

Simultaneous *in vivo* recordings of pectoralis force, fascicle length change and muscle activation (EMGs) show consistent patterns of length oscillation at both anterior and posterior sites with respect to muscle activation and force development (Fig. 2). Length changes of the muscle correspond to the oscillatory motion of the wing during the upstroke and downstroke. Because the upstroke is more rapid, the oscillatory pattern of length change is asymmetrical, so that muscle lengthening occurs over 37±3 % of the wingbeat cycle and muscle shortening over 63±3 % of the cycle (means ± S.D. for all five birds, N=144 total wing beats; Fig. 3). The pectoralis exerts force over much of the shortening (downstroke) phase of each wingbeat cycle. Muscle shortening velocities were greatest during the middle of the downstroke, averaging 7.01±1.29 lengths s^{-1} at the anterior site and 6.37±1.68 lengths s^{-1} at the posterior site (N=35, pooled for all animals), being much lower early (anterior 2.49±1.18 lengths s^{-1}, posterior 3.98±2.24 lengths s^{-1}, N=35) and late (anterior 2.63±1.09 lengths s^{-1}, posterior 2.81±0.75 lengths s^{-1}, N=35) in the downstroke. Overall, muscle shortening velocities averaged 5.38±1.33 lengths s^{-1} at the anterior site and 4.88±1.27 lengths s^{-1} (N=35) at the posterior site during the downstroke.

In general, maximal muscle lengthening is quite uniform on a cycle-by-cycle basis, with more variable changes in shortening observed at the end of the downstroke. Just prior to take-off, the birds generally elevated their wings in anticipation of being released. The recordings also show that

the birds generally maintained their wings in a more elevated position (greater muscle lengths) as they landed, progressively restricting downstroke movements to control their stall at the perch (Fig. 2). Typically, 8–10 wing beats were selected for analysis from the middle portion of the flight sequence because the birds settled into steady flight at a speed of approximately 5–6 m s^{-1} and a mean wingbeat frequency of 8.7 Hz (Table 2) during this time. Characteristic of slow flight, the birds flew using a 'figure-of-eight' wing tip reversal pattern (Brown, 1948), hypothesized to be a vortex ring gait (Tobalske and Dial, 1996), with their tails depressed and flared. Their body angle relative to the horizontal averaged 32±5 °, with the stroke
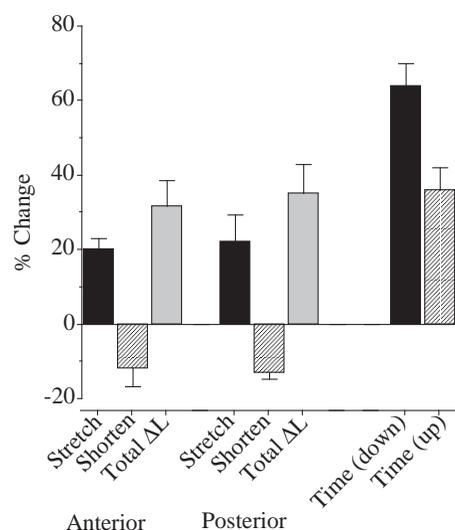

Fig. 3. Histogram showing pooled comparisons of fractional muscle fascicle lengthening (stretch), shortening (shorten) and net shortening (total Δ*L*) for the anterior and posterior recording sites, as well as upstroke (time up) and downstroke (time down) durations. Values are means ± S.D. (N=144 wing beats from five birds).

Table 2. *Summary of muscle force, (net) work per cycle and mean muscle power*

| Animal | Frequency (Hz) | Peak force (N) | Muscle work (J kg^{-1} muscle) | | N | Mean muscle power (W kg^{-1} muscle) |
			Anterior	Posterior		
1	8.38	45.3±4.0	6.2±0.7	11.2±1.3	25	72.6
2	8.66	53.0±2.1	11.7±2.9	14.9±1.9	33	115.2
3	8.96	39.2±2.2	7.6±0.7	5.3±0.4	24	57.7
4	8.98	43.3±2.5	14.0±2.6	10.8±1.8	23	111.3
5	8.53	55.6±2.6		10.9±1.1	39	93.0*
Mean	8.70±0.26	47.3±6.8	9.9±3.4	10.6±3.6		90.0±24.7

Values are means ± S.D.
*Calculated on the basis of work measured at the posterior site only.

plane angle of the wing relative to the body being 72±6 ° (*N*=10 flights).

Expanded sequences of muscle force and length change for two of the pigeons (Fig. 4) show that the pectoralis begins to develop force near the end of the upstroke, just before muscle length change reverses direction to start the downstroke. Muscle force then peaks approximately 35–40 % of the way through the downstroke (when the wing is elevated approximately 45 ° above horizontal; Dial and Biewener, 1993). Although the magnitude of muscle length change is not uniform at the anterior and posterior sites, the timing of muscle lengthening and shortening is very similar (posterior length changes averaged 3.4±2.5 ms delay relative to anterior length changes, *N*=117 wing beats pooled for four birds). In the four birds for which anterior and posterior length recordings were made, differences in fascicle length change (strain) measured between the sites ranged from as little as 2 % (pigeon 4) to as

much as 27 % (pigeon 1), averaging 19±12 %. In three of the four birds, these differences were statistically significant (paired *t*-test, *P*<0.001, *N*=20 for each bird).

Timing of muscle activation, muscle force and fascicle length change

Neural activation of the pectoralis (EMG onset) preceded the onset of force development by 9±5 ms (*N*=44) at the anterior recording site and by 5±4 ms (*N*=38) at the posterior recording site, ceasing 13±9 ms (average for the two sites) after the time when force reached a maximum (Fig. 5; see also Fig. 9). The delay in the onset of posterior EMG activity was consistent with the slight delay in posterior fascicle length changes relative to anterior length changes, but these differences were not significant (*P*>0.05). Both the onset of EMG activity and start of force development preceded muscle shortening (and by implication the beginning of the downstroke) by a few

Fig. 4. Expanded wingbeat cycles for pigeons 1 (the tenth cycle shown in Fig. 2) and 2, showing muscle force relative to fractional length changes of the anterior and posterior fascicles. One complete cycle is shown, beginning at the onset of muscle shortening (the approximate timings of the downstroke and upstroke are indicated above together with wingbeat frequency). Fractional length changes are superimposed to show the similar timing and pattern of muscle length change at these two locations, despite differences in their magnitude. Muscle lengthening during the upstroke occurs more rapidly than muscle shortening during the downstroke. Muscle force peaks early in the downstroke. Consequently, the pectoralis shortens over most of the period of force generation. DPC, deltopectoral crest.
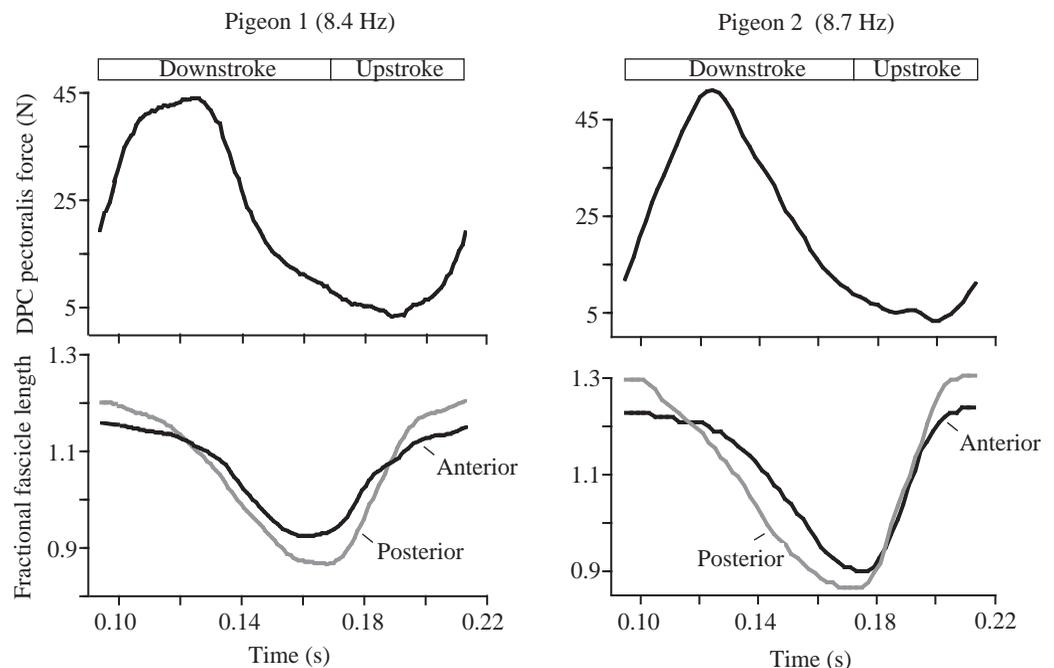
milliseconds (14 ms and 17 ms, respectively, based on the average timing of anterior and posterior fascicles). In many cases, therefore, the pectoralis developed force while still being stretched near the end of the upstroke, just prior to shortening. Nevertheless, most of its stretching during the upstroke was passive, occurring when force was near zero. Increases in muscle fascicle length generally occurred at lengths much greater than the resting length recorded at the end of the flight sequence (Fig. 2, but see also Figs 3, 5, 6). Consequently, net shortening of the pectoralis was less than that for lengthening relative to resting length. On average, the anterior and posterior muscle fascicles lengthened to 120±5 % of their resting length before shortening to 88±4 % of their resting length, resulting in a total strain amplitude of 32±8 % (anterior, *N*=144; posterior, *N*=117; Fig. 3). This extensive shortening is consistent with the role of the muscle in generating mechanical power by wing depression at the shoulder (approximately 80–90 °) during the downstroke.

In vivo *work loops and mechanical power output*

Plotting synchronous recordings of muscle force *versus* fascicle length yields *in vivo* work loops for the pectoralis during flight (Fig. 6). The regular pattern of muscle length change and force development over the middle part of the flight sequence results in consistent counterclockwise (positive) cycles of work output at both muscle sites. Differences in the shape of the work loops obtained at the anterior and posterior sites within a muscle are due to differences in the length changes of the fascicles recorded at these two locations (both use the same force pattern recorded at the DPC). Variation in work loop shape among animals, however, mainly reflects differences in the pattern of DPC strain that was recorded to measure muscle force in the different animals (compare, for example, the force traces shown for pigeons 1 and 2 in Fig. 4 and pigeon 2 in Fig. 5A). This probably results from small differences in strain gauge location and alignment on the DPC that contribute to differences in the pattern of strain recorded
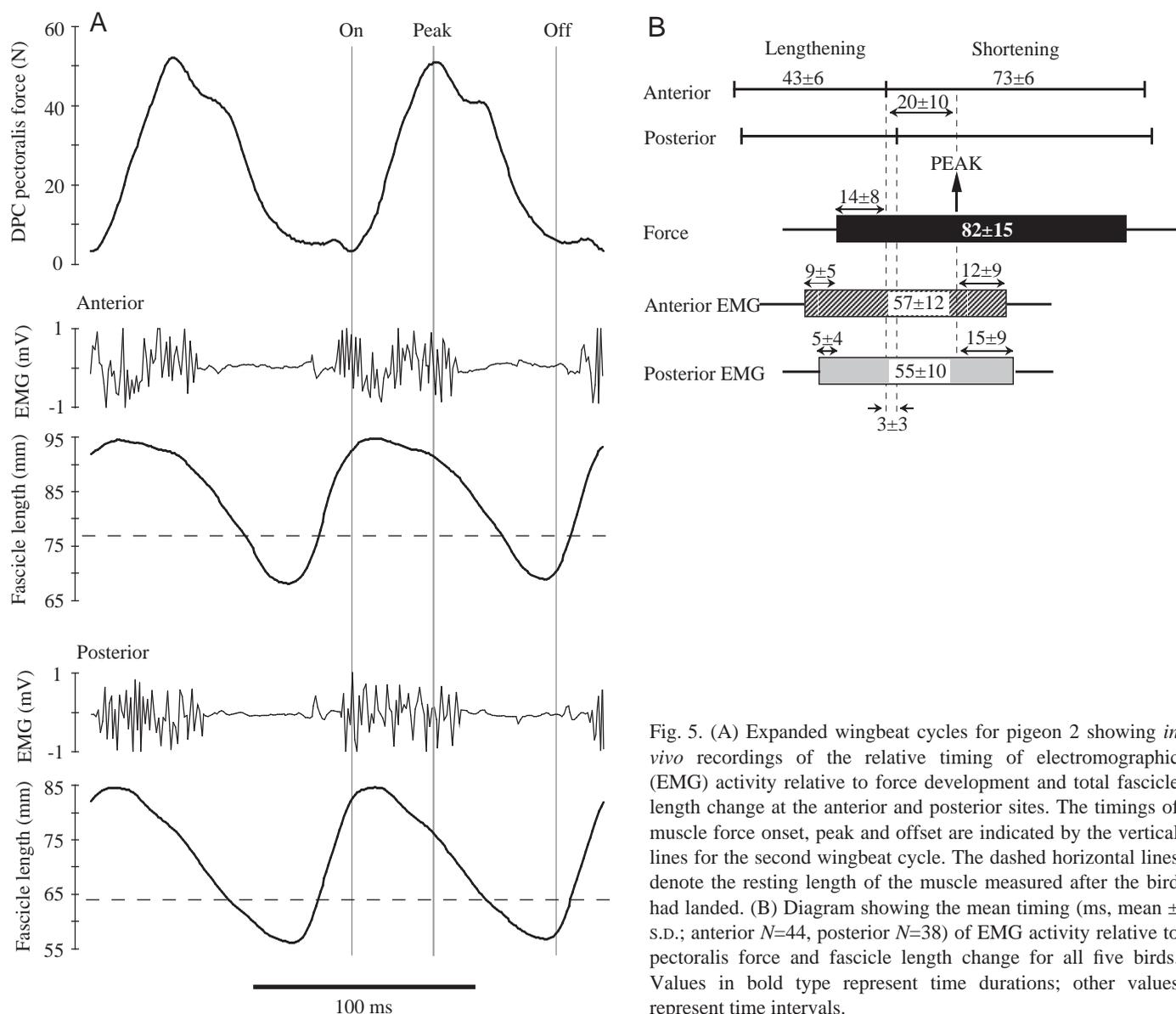

Fig. 5. (A) Expanded wingbeat cycles for pigeon 2 showing *in vivo* recordings of the relative timing of electromographic (EMG) activity relative to force development and total fascicle length change at the anterior and posterior sites. The timings of muscle force onset, peak and offset are indicated by the vertical lines for the second wingbeat cycle. The dashed horizontal lines denote the resting length of the muscle measured after the bird had landed. (B) Diagram showing the mean timing (ms, mean ± S.D.; anterior *N*=44, posterior *N*=38) of EMG activity relative to pectoralis force and fascicle length change for all five birds. Values in bold type represent time durations; other values represent time intervals.

Anterior   Posterior
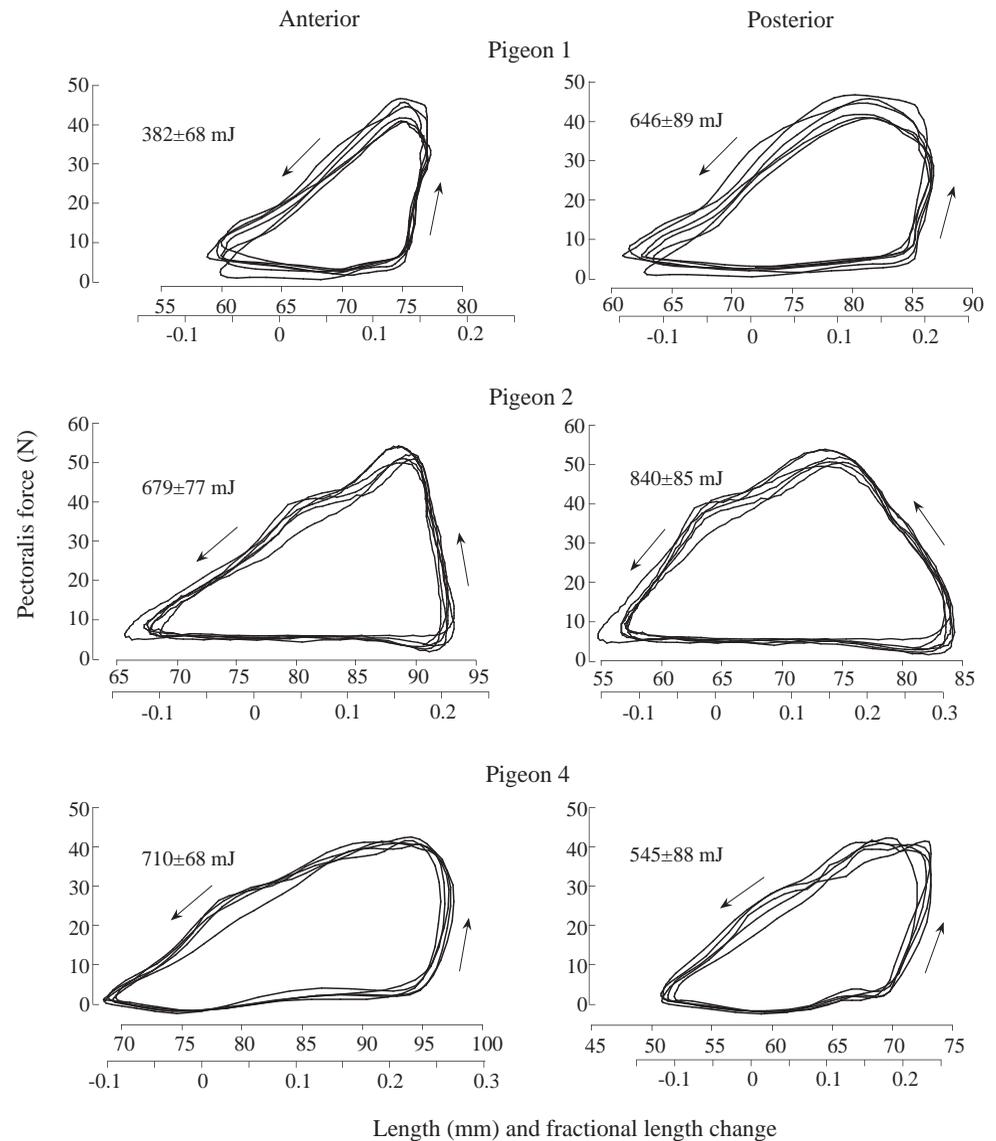
Pigeon 1

Pigeon 2

Pectoralis force (N)

Pigeon 4

Fig. 6. Graphs of five consecutive *in vivo* work loops obtained from the anterior and posterior regions of the pectoralis for three of the pigeons (1, 2 and 4) during the middle portion of their flight sequence. Arrows indicate the direction of force and length changes. The mean value (±S.D.) of net work (the area within the loop) is given for each set of loops. See text for further details.

Length (mm) and fractional length change

and used to measure pectoralis force. In contrast, the oscillatory pattern of length change shown in Fig. 2 was observed consistently in all animals.

In general, the fascicles develop force isometrically or are actively stretched to a small degree near the end of the upstroke. Force then develops more slowly as the wing reverses direction and begins the downstroke. Although muscle force declines with continued shortening, it is maintained throughout the downstroke. The initial decline in force during shortening coincides with an increase in shortening velocity (force–velocity effects). Note that in Fig. 5A there is little decrease in force while the velocity remains fairly constant. The subsequent decline in force also corresponds with the end of muscle activation, which ceases shortly after the peak in muscle force (Fig. 5, see also Fig. 9). In all birds, pectoralis force declines to near zero before the fascicles begin to lengthen at the start of the succeeding upstroke. Consequently, the amount of negative work absorbed by the pectoralis is small compared with the positive work that it performs when

shortening. This results in considerable net work (the area within the loop) done during each wingbeat cycle.

Although the magnitude of force generated by the pectoralis varies considerably over the entire flight sequence (Fig. 2), work loops produced by the muscle at the anterior and posterior sites are consistent in shape when differing cycles within the sequence are compared (Fig. 7). Except for the terminal wingbeat cycle(s), as the bird goes into a stall to land, the pectoralis performs a substantial amount of net positive work (85±28 %) relative to the amount absorbed as negative work (15±10 %). This is most clearly observed in Fig. 8, which shows a representative sample of the positive work, negative work and net work performed by pigeon 5 on a cycle-by-cycle basis over an entire flight sequence.

Combining the *in vivo* muscle work loops generated by the anterior and posterior pectoralis fascicles with the timing of EMG activity (Fig. 5B) allows the relative phase of neural activation to be depicted within the work loop cycle (Fig. 9). Consistent with the timings shown in Fig. 5B, neural activation

Pigeon 1

Pigeon 2

Anterior
● 248 mJ
Posterior
○ 457 mJ

Cycle 2

Anterior
● 406 mJ
Posterior
○ 655 mJ

Cycle 1

Cycle 5

● 324 mJ

○ 614 mJ

Cycle 5

● 509 mJ

○ 786 mJ

Pectoralis force (N)

Cycle 10

● 371 mJ
○ 712 mJ

Cycle 10
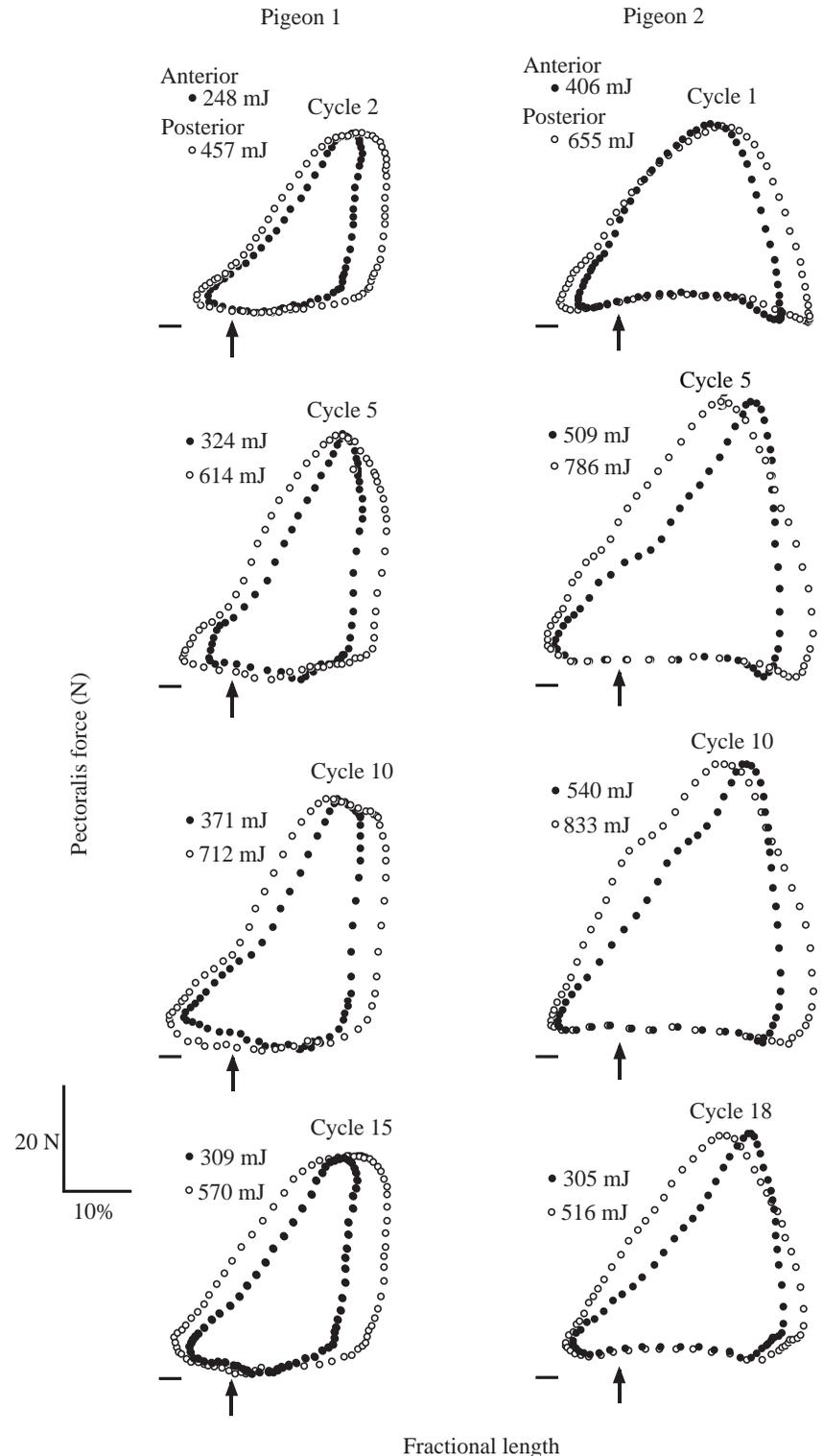
● 540 mJ

○ 833 mJ

20 N

10%

Fig. 7. Work loops obtained for pigeons 1 and 2 at two different sites in the pectoralis muscle and for four different cycles during a flight sequence, showing that, despite changes in magnitude, the force–length behavior of the pectoralis was consistent over successive wingbeat cycles. Fractional length changes of the muscle are shown, with the arrows indicating the resting length of the muscle fascicles (determined at the end of the flight sequence, see Fig. 2). Small horizontal marks denote zero force. The net positive work performed based on the length changes recorded from the anterior (open circles) and posterior (filled circles) sites are shown for each cycle.

Cycle 15

● 309 mJ
○ 570 mJ

Cycle 18

● 305 mJ

○ 516 mJ

Fractional length

precedes the development of force, while the muscle's fascicles are still lengthening, and continues throughout the full development of force. Muscle activation is therefore phase-advanced by 18 %, and the onset of force development is phase-advanced by 12 %, with respect to the onset of muscle shortening being the start of the work loop cycle. Activation ends just after peak force is developed by the muscle (30 %

into the shortening phase of the cycle). This allows the muscle to relax to nearly zero force by the end of the downstroke, enabling the muscle to be lengthened with little loss of power during the upstroke.

Peak force and mass-specific muscle work and power

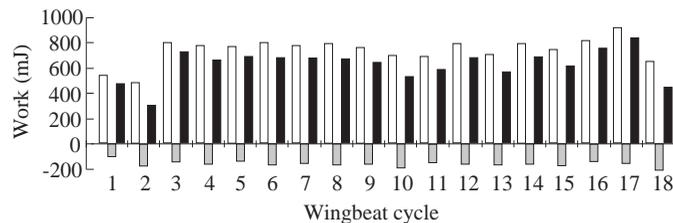Peak forces produced by the pigeon pectoralis, under the

Fig. 8. Histogram showing the positive work (open columns), negative work (shaded columns) and net work (black columns) generated during successive wingbeat cycles of a flight sequence by pigeon 5.
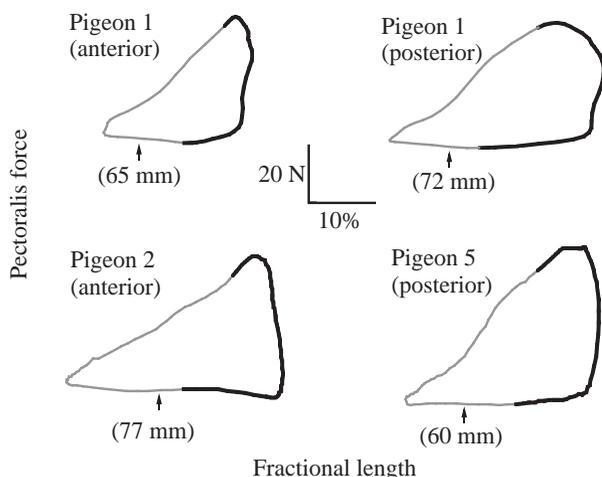

Fig. 9. Representative work loops showing the relative phase of electromyographic activation (bold dark lines) of the muscle fibers relative to muscle force development and fractional length change. The resting length (given in parentheses) is denoted by the arrow in each case.

recorded conditions of steady slow forward flight, averaged 47.2±6.8 N (N=144). These forces correspond to a mean net muscle mass-specific work of 9.9±3.6 J kg^{-1} at the anterior site and 10.6±3.4 J kg^{-1} at the posterior site (Table 2). Differences in muscle work and mechanical power output among the five birds were generally associated with differences in wing loading and disk loading (Table 1). Pigeon 3 had the lowest disk loading, and its pectoralis generated the least mechanical power for its size; pigeons 2 and 4 had the highest wing and disk loading, and their pectoralis muscles generated the greatest mass-specific power. Averaging muscle work for these two sites and multiplying by wingbeat frequency gives a muscle mass-specific net mechanical power output of 90.0±24.7 W kg^{-1} (Table 2). However, because the fascicle length of the muscle at these sites is greater than at other sites, this overestimates the power output for the pectoralis as a whole. Assuming that the mean fractional length change obtained for these two sites is representative for all active fascicles within the muscle and using a value of 55 mm for the mean fascicle length of the pectoralis gives a more reliable estimate of 70.2 W kg^{-1} as the overall mass-specific net power

output of the muscle. Accounting for both pectoralis muscles, but neglecting contributions from other muscles to mechanical power output, yields a net power output of 12.6 W kg^{-1} body mass for the entire animal.

Discussion

In vivo *work loop recordings*

A principal goal of our study was to use direct measurements of the force and length changes of the pigeon pectoralis to characterize its work performance during steady forward flight. These recordings allow us to confirm earlier results (Dial and Biewener, 1993), which were based on kinematic estimates of muscle length change in combination with DPC force recordings. The work loops that we obtain here represent the first complete *in vivo* work loops described for a flying animal. These work loops revise (somewhat) the shape of the work loops produced by the pectoralis previously reported on the basis of wing kinematics. They show less active lengthening of the pectoralis at the end of the upstroke and a more rapid decline in muscle force during shortening. A decline in muscle force during shortening is often observed in work loops produced by other skeletal muscles (Josephson, 1985; Stevens, 1988; Stevenson and Josephson, 1990) or muscle fiber bundles (Altringham and Johnston, 1990; Barclay, 1994; Curtin and Woledge, 1993) when stimulated to perform work under *in vitro* conditions of sinusoidal length oscillation or to simulate *in vivo* contractile conditions of power ouput (Lutz and Rome, 1994; Rome *et al.* 1993). It is the case, however, that work loop shape can vary considerably depending on cycle frequency and phase of stimulation, as well as function. The work loops generated by the pigeon pectoralis for mechanical power during flight are quite distinct from the force–length behavior of leg muscles in hopping wallabies *Macropus eugenii* (Biewener *et al.* 1998; Biewener, 1998) and running turkeys *Meleagris galapavo* (Roberts *et al.* 1997), which generate force with little change in length.

For both the *in vivo* work loops generated by the pigeon pectoralis and the *in vitro* work loops driven by sinusoidal length oscillations, muscle work is enhanced by the rapid development of force under nearly isometric or active lengthening conditions, followed by muscle shortening throughout most of the period of active force generation. These are the conditions under which *in vitro* work loop studies have found that skeletal muscles generate maximal power (e.g. Altringham and Johnston, 1990; Askew and Marsh, 1997; James *et al.* 1995; Swoap *et al.* 1993). Unlike the symmetrical sinusoidal length oscillations typical of most *in vitro* studies, however, our sonomicrometry recordings show that the length changes of the pigeon pectoralis are asymmetrical during flight, so that lengthening occurs more rapidly over approximately one-third of the cycle, allowing shortening to occur over nearly two-thirds of the cycle. Askew and Marsh (1997) have recently shown that, when length changes are altered to allow a longer shortening phase (75 % *versus* 50 % of the cycle), *in vitro* work and power output of mouse soleus

and extensor digitorum longus muscles are increased by 38 % compared with when the imposed length changes are symmetrical. Their results were obtained by comparing sawtooth length trajectories of the muscle (symmetrical sinusoidal length oscillations yielded approximately 8 % less mechanical power compared with symmetrical sawtooth length changes). The increase in muscle work and power output at longer shortening phases results from both an increase in shortening distance and an increase in force development by the muscles. However, because of their discontinuous nature, sawtooth length trajectories cannot accurately represent how muscles operate under real biological conditions. We find here that the pigeon pectoralis operates with a similarly long shortening phase *in vivo*, but with continuous length changes that exhibit an asymmetrical pattern. An increased period of shortening probably allows the muscle to become more fully activated or to be active for longer in order to develop greater force, while shortening at a velocity that may enhance its power output (Askew and Marsh, 1997). To confirm whether this is the case, it will be necessary to use the work loop technique to study the mechanical performance of pectoralis fasicles under *in vitro* conditions of varying length change trajectories. By shortening over a longer fraction of the cycle, however, the muscle must be able to deactivate quickly enough so that it can be lengthened in a nearly relaxed state. The pigeon pectoralis appears to be able to accomplish this with a nearly 2:1 phase ratio of shortening *versus* lengthening.

Muscle length changes and wing kinematics

Consistent work loop patterns were observed among animals and over nearly the full sequence of flight. The regular excursions of the muscle length changes (Fig. 2) and work loop patterns (Figs 6, 7) reflect the regular wingbeat pattern of the birds under the recorded conditions of slow steady forward flight. Whereas pectoralis fascicles were stretched to a uniform maximum length at the end of each upstroke, greater variation was observed in the degree to which the muscle shortened during the downstroke. These recordings are consistent with the elevation of the shoulder at the end of the upstroke being limited by the range of motion of the wings to a near vertical position, as they approach contact with each other, with wing depression at the end of the downstroke being a more variable component of flight behavior. The greatest variation in muscle length (and by implication wing position) occurred near the end of the flight, as the bird landed, with subsequent downstrokes becoming progressively more restricted (Fig. 2). Future studies that incorporate improved kinematic data with sonomicrometry recordings are needed to confirm how pectoralis length changes are associated with more detailed aspects of wing movement.

During slow forward flight, the distal end of the wing is swung forward late in the downstroke as the elbow and wrist flex and the wings are supinated, being brought together beneath and in front of the animal (Brown, 1948). This results in a wing tip reversal as the wing begins the upstroke, which may allow the wing to produce limited thrust during the upstroke (Aldridge, 1986; Warrick and Dial, 1998) and to initiate recovery from a turn (Warrick and Dial, 1998). However, during the 'forward swing' of the distal wing, further depression of the wing at the shoulder appears to be limited (Brown, 1948). Our sonomicrometry recordings suggest that this is the case, because the muscle's rate of shortening slows late in the downstroke before it is lengthened. Prior to this, muscle shortening is rapid and more uniform, reflecting wing depression at the shoulder until just after the wing passes below horizontal.

In contrast to the development of peak force in the first half of the downstroke, we find that peak strain develops in the shafts of primary flight feathers late in the downstroke, at a time when the wing undergoes its forward swing (Corning and Biewener, 1998). The timing of pectoralis force and feather strain relative to aerodynamic force production is of key interest. The earlier timing of force generation by the pectoralis suggests that, for slow flight, the majority of aerodynamic force is produced during the first three-quarters of the downstroke before the wing reaches a horizontal position. High pectoralis force is also required early in the downstroke to accelerate the wing. Useful aerodynamic force production when the wings are subsequently swung forward, so that their ventral surfaces oppose each other, seems unlikely. The later development of peak feather strain, therefore, may result from a distal shift in the local center of lift force acting on individual flight feathers (which will produce a larger bending moment and, hence, greater strain at the feather's base) as the wing is swept forward and the flight primaries are spread (Corning and Biewener, 1998).

Muscle length change in relation to muscle work

The sonomicrometry recordings show that the pigeon pectoralis first lengthens to 120 % its resting length and then shortens to 88 % of its resting length while generating force, resulting in a total strain amplitude of 32 %. Although we do not know how these length changes relate to this muscle's active force–length properties, such length changes are generally greater than those commonly considered to be favorable to a muscle's ability to generate force and to do work. When muscles are studied under either quasi-static or *in vitro* work conditions, length changes are often maintained within short ranges (±5 %) of a muscle's resting or optimum isometric length (L_0). Our recordings of the pigeon pectoralis indicate that the degree of muscle shortening is much greater than this during flight. By shortening by a greater fraction of its resting length, the muscle is able to do more work on a cycle-by-cycle basis. At the same time, the pectoralis is able to accomplish this at a high frequency. The longer time period in the wingbeat cycle available for shortening probably facilitates the muscle's work output. Muscle stretch well beyond optimal length (L_0) for isometric tension development is often interpreted as an unstable and potentially damaging range of length for a muscle because it positions the muscle's sarcomeres on the descending limb of their length–tension curve (Gordon *et al.* 1966). Consequently, it will be interesting

to learn how the resting length of the pectoralis compares with its L_0 and whether the extensive stretch that we observe beyond the muscle's resting length correlates with lengths that are on the descending limb of the muscle's active length–tension curve. If this is the case, it seems likely that passive contributions to muscle stiffness would be important for the muscle to operate at such great lengths.

Earlier estimates of mechanical work and power output in wild-type pigeons determined from kinematic analysis of wing elevation and the muscle's moment arm at the shoulder (Dial and Biewener, 1993) yielded similar estimates of muscle strain amplitude during steady flight (32 %, based on maximum and minimum lengths of 107 % and 75 % relative to resting length) but greater estimates during ground take-off (53 %, based on maximum and minimum lengths of 116 % and 63 % relative to resting length). These kinematic measurements of muscle length change probably underestimated the degree of fascicle lengthening *versus* shortening (relative to rest) because they were based on *post-mortem* measurements of fascicle length rather than *in vivo* changes in muscle length that can be determined using sonomicrometry. Kinematic analysis of muscle length change and work is always limited by the assumption of uniform length change of all activated fibers within the muscle, as well as by uncertainty concerning the length change of the tendon *versus* the muscle fibers with respect to calculated overall muscle–tendon length changes. In the case of the avian pectoralis, this latter concern is not a problem because of its extremely short tendon. Our measurements of fascicle length change at two sites within the sternobrachial portion of the pigeon pectoralis show, however, that the former assumption can be a problem. Despite similarities in the timing of length change and neural activation at the anterior and posterior sites, differences in fascicle length change averaged 19 % in the four birds for which measurements were obtained at these two sites. Because of this, as well as differences in fascicle length, muscle work differed by as much as 44 % at the anterior and posterior recording sites in one bird (pigeon 1) and averaged 14 %.

Consequently, while our recordings show consistent force–length behavior of the fascicles in these two regions, they also warrant caution regarding assumptions of uniform function of fibers throughout a muscle. This is particularly important when a muscle, such as the pectoralis, has an expansive origin (or insertion) with fibers of varying length and orientation. Future studies that sample muscle fiber or fascicle length changes at multiple sites within a muscle will help to clarify the possible significance of such differences. The present study confirms the results of Boggs and Dial (1993), who found a temporal pattern of motor activation within the pectoralis in which more anterior regions of the sternobrachial portion of the muscle were activated slightly prior to more posterior regions, with fibers in the thoracobrachial portion of the pectoralis being the last to exhibit EMG activity (in a reverse posterior-to-anterior sequence). Our data suggest that slight delays in EMG onset correspond with comparable delays in fascicle length change; however, such differences were not statistically significant across the entire data sample. The relative delay in muscle activation and shortening of more posterior portions of the pectoralis may be related to its role in pronation of the wing during the later stages of the downstroke. Boggs and Dial (1993) suggested that regional variation in activation and force development may allow the pectoralis to vary the direction of applied force to the humerus over the course of the downstroke. More detailed analyses of wing kinematics and muscle length change are needed to determine whether this is the case. Nevertheless, despite the observed differences in the relative magnitude of length change, the generally consistent contractile behavior of the anterior and posterior fascicles lends support to functional interpretations of the muscle's role in generating mechanical power for aerodynamic lift.

The greatest difference between our sonomicrometry measurements of *in vivo* work loops and those obtained from kinematic estimates of muscle length change (Dial and Biewener, 1993) is their shape. Whereas our earlier estimates showed an almost circular work loop, the *in vivo* recordings show that force declines more rapidly as the muscle shortens, reducing the area within the work loop. This decline in force, however, favors the muscle's ability to relax before being subsequently stretched, which would otherwise require increased antagonistic work. Such a decay in force is also commonly observed under *in vitro* work loop conditions (Altringham and Johnston, 1990; Barclay, 1994; Curtin and Woledge, 1993; Rome *et al.* 1993; Stevens, 1988; Stevenson and Josephson, 1990). Our earlier kinematic estimates of length change also suggested greater negative work during active lengthening of the pectoralis late in the upstroke compared with the work loops presented here. While the *in vivo* work loops generally indicate active lengthening of the pectoralis (four of five birds), the amount of negative work required to decelerate the wing at the end of the upstroke is probably smaller than previously estimated.

The Silver King is a large racing breed of pigeon. Consistent with their 2.1-fold greater body mass, the Silver King pigeons generated peak pectoralis forces (47.3 N) that were 2.4 times greater than those measured from wild-type pigeons (19.7 N; body mass 307 g) under similar conditions of steady forward flight (Dial and Biewener, 1993). Our sonomicrometry measurements indicate a muscle mass-specific net power of $70 \, \text{W} \, \text{kg}^{-1}$, exceeding the value of $51 \, \text{W} \, \text{kg}^{-1}$ that we obtained from our previous kinematic estimates of muscle length change in wild-type pigeons. This difference reflects both an increase in muscle strain obtained using sonomicrometry (28 %) and an increase in muscle stress (45 %). For its size, the Silver King has a smaller pectoralis than the wild-type pigeons (9.0 % *versus* 9.9 % of body mass) used in our earlier study, resulting in a smaller cross-sectional area relative to the forces produced during slow level flight. The increase in muscle work resulting from greater muscle strain and stress is diminished, however, by the less rounded work loop shape that was recorded *in vivo*.

Our estimate of mass-specific net muscle power obtained here is still lower than the estimate ($110 \, \text{W} \, \text{kg}^{-1}$) determined

from Pennycuick's (1968) analysis of pigeon flight, based on steady-state (actuator disk) aerodynamic theory. In a subsequent theoretical analysis of the power requirements for flight based on vorticity generated in the wake of a flying animal, Rayner (1979) predicted a lower value for pigeons, which we calculate to be 87 W kg^{-1} at a speed of approximately 5–6 m s^{-1} (assuming a similar total pectoralis mass equal to 20 % of body mass). Subsequent vortex visualization analyses of slowly flying pigeons (Spedding *et al.* 1984) and jackdaws (*Corvus monedula*; Spedding, 1986), using a discontinuous vortex ring gait, calculated power requirements that were as much as 50–65 % lower than predicted by the theory. However, measurements made of kestrels (*Falco tinnunculus*; Spedding, 1987) flying at approximately 7 m s^{-1}, using a continuous vortex gait, were found to underestimate the induced power predicted by actuator disk theory (Pennycuick, 1975) by only 16 %. Given that our *in vivo* measurements of power output are still approximately 24–50 % lower than those predicted by theory, it seems likely that non-steady effects that allow for improved aerodynamic performance, particularly at low speeds, are important in the flapping flight of birds. Such non-steady effects appear to be important to the lift generation of flying insects (Dickinson, 1996; Ellington *et al.* 1996; Lui *et al.* 1998). Consistent with this, our recent analysis of the mechanical power output of black-billed magpies flying in a wind tunnel over a range of steady speeds (Dial *et al.* 1997) indicates that the prediction of a 'U'-shaped power curve by classical aerodynamic theory can be misleading. It appears that magpies modulate their flight behavior in such as way as to be able to fly over a wide range of speed (4–14 m s^{-1}) with little change in mechanical power requirement. The results for magpies, however, also rely on kinematic estimates of muscle length change, for which muscle shortening averaged 25 % of resting length, a value similar to our kinematic estimates of length change in wild-type pigeons. Consequently, these results would also benefit from direct measurements of muscle length change in order to confirm work loop shape and power output under *in vivo* flight conditions.

Comparison of muscle force–length properties under differing functional activities

In contrast to the pigeon pectoralis and other muscles designed to generate mechanical power, such as those that power a frog's jump (Calow and Alexander, 1973; Lutz and Rome, 1994) or a fish's swimming (Altringham and Johnston, 1990; Rome *et al.* 1993), which produce large counterclockwise (positive) work loops, certain leg muscles of running and hopping terrestrial animals appear to produce relatively little power. By contracting either isometrically or while being stretched, these muscles generate large forces but perform little net work. Direct recordings of force and length change within the lateral gastrocnemius muscle of running wild turkeys (*Meleagris galapavo*; Roberts *et al.* 1997) and the lateral gastrocnemius and plantaris muscles of tammar wallabies (*Macropus eugenii*; Biewener *et al.* 1998) show that these muscles generate forces that can exceed their peak

isometric force at faster speeds yet undergo very small strains (from <2 % to <6 %). It has been argued that the function of these muscles is to facilitate elastic energy storage and recovery in their tendons, at the same time reducing the amount of metabolic energy expended by the muscle to generate force (shorter fibers can generate force more economically than longer fibers because fewer cross-bridges are formed). On the basis of morphological evidence alone, a similar role has been ascribed to the highly pennate, short-fibered muscles of ungulates (Biewener, 1998; Dimery *et al.* 1986*a,b*; Ker *et al.* 1986), whose leg muscles appear most specialized for this task.

The avian pectoralis, in contrast, possesses long fascicles with only moderate pennation that insert directly on, or *via* short connective tissue aponeuroses, to the deltopectoral crest. In addition, there is growing evidence that the fascicles are made up of serially interdigitated fibers (Gaunt and Gans, 1993; Sokoloff *et al.* 1998; Trotter and Purslow, 1992; Trotter *et al.* 1992). A recent neuromuscular study (Sokoloff *et al.* 1998) indicates that motor units within different regions of the pectoralis may correspond to those regions that are recruited in a regular order during steady flight (Boggs and Dial, 1993), but motor units often may not span the entire length of the fascicle. Consequently, the implications of serial fiber organization remain unclear in terms of the neural control of pectoralis function and mechanisms of force transmission from the muscle's orgin to its insertion on the humerus at the DPC. Ultrastructural evidence suggests that force may be transferred by shear to parallel connective tissue elements surrounding individual fibers (Trotter and Purslow, 1992). Whatever the mechanism, it is clear that the pectoralis effectively transmits force to the DPC while shortening over a considerable distance to depress the wing. The long length of its fascicles facilitates this task. In contrast to the leg muscles of running and hopping animals, however, the pectoralis generates forces that are only 30 % of its peak isometric force during steady flight, increasing to 39 % during vertically ascending flight (Dial and Biewener, 1993; in the Silver King, we estimate that these forces may be 43 % and 57 %, respectively, of peak isometric force). This indicates that proportionally more fibers must be recruited within the pectoralis to generate a given level of force during flight, compared with a leg muscle that generates force isometrically in order to facilitate energy savings within a tendon spring. These differences reflect the classical trade-off in muscle architecture for force generation *versus* work and shortening.

References

ALDRIDGE, H. D. J. N. (1986). Kinematics and aerodynamics of the

greater horseshoe bat, *Rhinolophus ferrumequinum*, in horizontal flight at various speeds. *J. exp. Biol.* **126**, 479–497.

Altringham, J. D. and Johnston, I. A. (1990). Scaling effects on muscle function: power output of isolated fish muscle fibres performing oscillatory work. *J. exp. Biol.* **151**, 453–467.

Askew, G. N. and Marsh, R. L. (1997). The effects of length trajectory on the mechanical power output of mouse skeletal muscles. *J. exp. Biol.* **200**, 3119–3131.

Barclay, C. J. (1994). Efficiency of fast- and slow-twitch muscles of mouse performing cyclic contractions. *J. exp. Biol.* **193**, 65–78.

Biewener, A. A. (1998). Muscle–tendon stresses and elastic energy storage during locomotion in the horse. *Comp. Biochem. Physiol.* B **120**, 73–87.

Biewener, A. A. and Baudinette, R. V. (1995). *In vivo* muscle force and elastic energy storage during steady-speed hopping of tammar wallabies (*Macropus eugenii*). *J. exp. Biol.* **198**, 1829–1841.

Biewener, A. A., Dial, K. P. and Goslow, G. E., Jr (1992). Pectoralis muscle force and power output during flight in the starling. *J. exp. Biol.* **164**, 1–18.

Biewener, A. A., Konieczynski, D. D. and Baudinette, R. V. (1998). *In vivo* muscle force–length behavior during steady-speed hopping in tammar wallabies. *J. exp. Biol.* **201**, 1681–1694.

Boggs, D. F. and Dial, K. P. (1993). Neuromuscular organization and regional EMG activity of the pectoralis in the pigeon. *J. Morph.* **218**, 43–57.

Brown, R. J. H. (1948). The flight of birds. The flapping cycle of the pigeon. *J. exp. Biol.* **7**, 322–333.

Calow, L. J. and Alexander, R. McN. (1973). A mechanical analysis of the hind leg of a frog (*Rana temporaria*). *J. Zool., Lond.* **171**, 293–321.

Corning, W. R. and Biewener, A. A. (1998). *In vivo* strains in pigeon flight feather shafts: implications for structural design. *J. exp. Biol.* **201**, 3057–3065.

Curtin, N. A. and Woledge, R. C. (1993). Efficiency of energy conversion during sinusoidal movement of white muscle fibers from the dogfish *Scyliorhinus canicula*. *J. exp. Biol.* **183**, 137–147.

Dial, K. P. (1992). Avian forelimb muscles and nonsteady flight: can birds fly without using the muscles of their wings? *Auk* **109**, 874–885.

Dial, K. P. and Biewener, A. A. (1993). Pectoralis muscle force and power output during different modes of flight in pigeons (*Columba livia*). *J. exp. Biol.* **176**, 31–54.

Dial, K. P., Biewener, A. A., Tobalske, B. W. and Warrick, D. R. (1997). Mechanical power output of bird flight. *Nature* **390**, 67–70.

Dickinson, M. H. (1996). The wake dynamics and flight forces of the fruit fly *Drosophila melanogaster*. *J. exp. Biol.* **199**, 2085–2104.

Dimery, N. J., Alexander, R. McN. and Ker, R. F. (1986*a*). Elastic extension of leg tendons in the locomotion of horses (*Equus caballus*). *J. Zool., Lond.* **210**, 415–425.

Dimery, N. J., Ker, R. J. and Alexander, R. McN. (1986*b*). Elastic properties of the feet of deer (Cervidae). *J. Zool., Lond.* **208**, 161–169.

Ellington, C. P. (1984). The aerodynamics of hovering insect flight. The quasi-steady analysis. *Phil. Trans. R. Soc. Lond. B* **305**, 1–15.

Ellington, C. P., van den Berg, C., Willmott, A. P. and Thomas, A. L. R. (1996). Leading-edge vortices in insect flight. *Nature* **384**, 626–630.

Gaunt, A. S. and Gans, C. (1993). Variations in the distribution of motor end-plates in the avian pectoralis. *J. Morph.* **215**, 65–88.

Goldman, D. E. and Hueter, T. F. (1956). Tabular data of the

velocity and absorption of high frequency sound in mammalian tissues. *J. acoust. Soc. Am.* **28**, 35–53.

Goldman, D. E. and Richards, J. (1954). Measurements of high-frequency sound velocity in mammalian soft tissue. *J. acoust. Soc. Am.* **26**, 981–983.

Gordon, A. M., Huxley, A. F. and Julian, F. J. (1966). The variation in isometric tension with sarcomere length in vertebrate muscle fibers. *J. Physiol., Lond.* **184**, 170–192.

Greenewalt, C. H. (1975). The flight of birds. *Trans. Am. Phil. Soc.* **65**, 1–67.

Griffiths, R. I. (1991). Shortening of muscle fibers during stretch of the active cat medial gastrocnemius muscle: the role of tendon compliance. *J. Physiol., Lond.* **436**, 219–236.

Hill, A. V. (1938). The heat of shortening and the dynamic constants of muscle. *Proc. R. Soc. Lond. B* **126**, 136–195.

James, R. S., Altringham, J. D. and Goldspink, D. F. (1995). The mechanical properties of fast and slow skeletal muscles of the mouse in relation to their locomotory function. *J. exp. Biol.* **198**, 491–502.

Josephson, R. K. (1985). Mechanical power output from striated muscle during cyclical contraction. *J. exp. Biol.* **114**, 493–512.

Ker, R. F., Dimery, N. J. and Alexander, R. McN. (1986). The role of tendon elasticity in hopping in a wallaby (*Macropus rufogriseus*). *J. Zool., Lond.* A **208**, 417–428.

Lui, H., Ellington, C. P., Kawachi, K., Van den Berg, C. and Willmott, A. P. (1998). A computational fluid dynamic study of hawkmoth hovering. *J. exp. Biol.* **201**, 461–477.

Lutz, G. J. and Rome, L. C. (1994). Built for jumping: the design of the frog muscular system. *Science* **263**, 370–372.

Machin, K. E. and Pringle, J. W. S. (1960). The physiology of insect fibrillar flight muscle. III. The effects of sinusoidal changes in length on a beetle flight muscle. *Proc. R. Soc. Lond. B* **152**, 311–330.

Marsh, R. L. and Olson, J. M. (1994). Power output of scallop adductor muscle during contractions replicating the *in vivo* mechanical cycle. *J. exp. Biol.* **193**, 139–156.

Marsh, R. L., Olson, J. M. and Guzik, S. K. (1992). Mechanical performance of scallop adductor muscle during swimming. *Nature* **357**, 411–413.

McMahon, T. A. (1984). *Muscles, Reflexes and Locomotion.* Princeton, NJ: Princeton University Press.

Norberg, U. M. (1990). *Vertebrate Flight: Mechanics, Physiology, Morphology, Ecology and Evolution.* Heidelberg: Springer-Verlag.

Norberg, U. M. and Rayner, J. M. V. (1987). Ecological morphology and flight in bats (Mammalia: Chiroptera): wing adaptations, flight performance, foraging strategy and echolocation. *Phil. Trans. R. Soc. Lond. B* **316**, 335–427.

Pennycuick, C. J. (1968). Power requirements for horizontal flight in the pigeon *Columba livia*. *J. exp. Biol.* **49**, 527–555.

Pennycuick, C. J. (1975). Mechanics of flight. In *Avian Biology*, vol. 5 (ed. D. S. Farner and J. R. King), pp. 1–75. London: Academic Press.

Pennycuick, C. J. (1989). *Bird Flight Performance. A Practical Calculation Manual.* Oxford: Oxford University Press.

Rayner, J. M. V. (1979). A new approach to animal flight mechanics. *J. exp. Biol.* **80**, 17–54.

Rayner, J. M. V. (1995). Dynamics of vortex wakes of swimming and flying vertebrates. In *Biological Fluid Dynamics*, *Society for Experimental Biology Symposium* **49** (ed. C. P. Ellington and T. J. Pedley), pp. 131–155. Cambridge: Company of Biologists Ltd.

Roberts, T. J., Marsh, R. L., Weyand, P. G. and Taylor, C. R.

(1997). Muscular force in running turkeys: the economy of minimizing work. *Science* **275**, 1113–1115.

ROME, L. C., SWANK, D. AND CORDA, D. (1993). How fish power swimming. *Science* **261**, 340–343.

SCHOLEY, K. D. (1983). Developments in vertebrate flight: climbing and gliding in mammals and reptiles and the flapping flight of birds. PhD thesis, University of Bristol.

SOKOLOFF, A. J., RYAN, J. M., VALERIE, E., WILSON, D. S. AND GOSLOW, G. E., JR (1998). Neuromuscular organization of avian flight muscle: morphology and contractile properties of motor units in the pectoralis (*pars thoracicus*) of pigeon (*Columba livia*). *J. Morph.* **236**, 179–208.

SPEDDING, G. R. (1986). The wake of a jackdaw (*Corvus monedula*) in slow flight. *J. exp. Biol.* **125**, 287–307.

SPEDDING, G. R. (1987). The wake of a kestrel (*Falco tinnunculus*) in flapping flight. *J. exp. Biol.* **127**, 59–78.

SPEDDING, G. R., RAYNER, J. M. V. AND PENNYCUICK, C. J. (1984). Momentum and energy in the wake of a pigeon (*Columba livia*) in slow flight. *J. exp. Biol.* **111**, 81–102.

STEVENS, E. D. (1988). Effect of pH and stimulus phase on work done by isolated frog sartorius muscle during cyclical contraction. *J. Muscle Res. Cell Motil.* **9**, 329–333.

STEVENSON, R. D. AND JOSEPHSON, R. K. (1990). Effects of operating frequency and temperature on mechanical power output from moth flight muscle. *J. exp. Biol.* **149**, 61–78.

SWOAP, S. J., JOHNSON, T. P., JOSEPHSON, R. K. AND BENNETT, A. F. (1993). Temperature, muscle power output and limitations on burst performance of the lizard *Dipsosaurus dorsalis*. *J. exp. Biol.* **174**, 185–197.

TOBALSKE, B. AND DIAL, K. P. (1996). Flight kinematics of black-billed magpies and pigeons over a wide range of speeds. *J. exp. Biol.* **199**, 263–280.

TROTTER, J. A. AND PURSLOW, P. P. (1992). Functional morphology of the endomysium in series fibered muscles. *J. Morph.* **212**, 109–122.

TROTTER, J. A., SALGADO, J. D., OZBAYSAL, R. AND GAUNT, A. S. (1992). The composite structure of quail pectoralis muscle. *J. Morph.* **212**, 27–35.

WARRICK, D. R. AND DIAL, K. P. (1998). Kinematic, aerodynamic and anatomical mechanisms in the slow, maneuvering flight of pigeons. *J. exp. Biol.* **201**, 655–672.

WEIS-FOGH, T. AND ALEXANDER, R. McN. (1977). The sustained power output from striated muscle. In *Scale Effects in Animal Locomotion* (ed. T. J. Pedley). London: Academic Press.